Design of plasmonic grating structures towards optimum signal discrimination for biosensing applications

Uwe Bog,[1,2,*] Klaus Huska,[2] Frieder Maerkle,[1] Alexander Nesterov-Mueller,[1] Uli Lemmer,[2] and Timo Mappes[1]

[1]*Institute for Microstructure Technology, Karlsruhe Institute of Technology (KIT), D-76128 Karlsruhe, Germany*
[2]*Light Technology Institute (LTI) and Center for Functional Nanostructures (CFN), Karlsruhe Institute of Technology (KIT), D-76128 Karlsruhe, Germany*
[*]*uwe.bog@kit.edu*

Abstract: Sensors based on surface plasmon resonances (SPRs) have proven themselves as promising devices for molecular investigations – still there is potential to determine the geometrical parameter set for optimal sensing performance. Here we propose a comprehensive design rule for one-dimensional plasmonic grating structures. We present an analytical approach, which allows for estimation of the grating parameters for best SPR coupling efficiency for any geometry and design wavelength. On the example of sinusoidal gratings, we expand this solution and discuss numerically and experimentally, how the grating modulation depth can be refined to achieve optimal signal resolution. Finally, we propose a benchmark factor to assess the sensor performance, which can be applied to any sensing scheme utilizing resonances, allowing for comparison of different technological platforms.

OCIS codes: (280.4788) Optical sensing and sensors; (280.1415) Biological sensing and sensors; (240.6680) Surface plasmons; (050.2770) Gratings; (000.3860) Mathematical methods in physics.

References and links

1. S. M. Borisov and O. S. Wolfbeis, "Optical biosensors," Chem. Rev. **108**(2), 423–461 (2008).
2. L. Nicu and T. Leichlé, "Biosensors and tools for surface functionalization from the macro- to the nanoscale: The way forward," J. Appl. Phys. **104**(11), 111101 (2008).
3. J. Homola, "Surface plasmon resonance sensors for detection of chemical and biological species," Chem. Rev. **108**(2), 462–493 (2008).
4. X. Fan, I. M. White, S. I. Shopova, H. Zhu, J. D. Suter, and Y. Sun, "Sensitive optical biosensors for unlabeled targets: a review," Anal. Chim. Acta **620**(1-2), 8–26 (2008).
5. P. V. Lambeck, "Integrated optical sensors for the chemical domain," Meas. Sci. Technol. **17**(8), R93–R116 (2006).
6. R. B. M. Schasfoort and A. J. Tudos, *Handbook of surface plasmon resonance* (RSC Publishing, 2008).
7. J. Homola, S. S. Yee, and G. Gauglitz, "Surface plasmon resonance sensors: a review," Sens. Actuators B Chem. **54**(1-2), 3–15 (1999).
8. J. N. Anker, W. P. Hall, O. Lyandres, N. C. Shah, J. Zhao, and R. P. Van Duyne, "Biosensing with plasmonic nanosensors," Nat. Mater. **7**(6), 442–453 (2008).
9. X. D. Hoa, A. G. Kirk, and M. Tabrizian, "Towards integrated and sensitive surface plasmon resonance biosensors: a review of recent progress," Biosens. Bioelectron. **23**(2), 151–160 (2007).
10. M. Sukharev, P. R. Sievert, T. Seideman, and J. B. Ketterson, "Perfect coupling of light to surface plasmons with ultra-narrow linewidths," J. Chem. Phys. **131**(3), 034708 (2009).
11. W. L. Barnes, T. W. Preist, S. C. Kitson, and J. R. Sambles, "Physical origin of photonic energy gaps in the propagation of surface plasmons on gratings," Phys. Rev. B Condens. Matter **54**(9), 6227–6244 (1996).
12. J. Dostalek, J. Homola, and M. Miler, "Rich information format surface plasmon resonance biosensor based on array of diffraction gratings," Sens. Actuators B Chem. **107**(1), 154–161 (2005).
13. Y. Nazirizadeh, U. Bog, S. Sekula, T. Mappes, U. Lemmer, and M. Gerken, "Low-cost label-free biosensors using photonic crystals embedded between crossed polarizers," Opt. Express **18**(18), 19120–19128 (2010).
14. C. Vannahme, S. Klinkhammer, M. B. Christiansen, A. Kolew, A. Kristensen, U. Lemmer, and T. Mappes, "All-polymer organic semiconductor laser chips: parallel fabrication and encapsulation," Opt. Express **18**(24), 24881–24887 (2010).

#165521 - $15.00 USD Received 26 Mar 2012; revised 20 Apr 2012; accepted 20 Apr 2012; published 2 May 2012

15. R. W. Wood, "On a remarkable case of uneven distribution of light in a diffraction grating spectrum," Philos. Mag. **4**, 396–402 (1902).
16. U. Fano, "The theory of anomalous diffraction gratings and of quasi-stationary waves on metallic surfaces," J. Opt. Soc. Am. **31**(3), 213–222 (1941).
17. R. Ritchie, E. Arakawa, J. Cowan, and R. Hamm, "Surface plasmon resonance effect in grating diffraction," Phys. Rev. Lett. **21**(22), 1530–1533 (1968).
18. M. G. Moharam and T. K. Gaylord, "Rigorous coupled-wave analysis of metallic surface-relief gratings," J. Opt. Soc. Am. A **3**(11), 1780–1787 (1986).
19. I. Baltog, N. Primeau, R. Reinisch, and J. L. Coutaz, "Surface enhanced Raman scattering on silver grating: optimized antennalike gain of the stokes signal of 104," Appl. Phys. Lett. **66**(10), 1187 (1995).
20. S. C. Kitson, W. L. Barnes, G. W. Bradberry, and J. R. Sambles, "Surface profile dependence of surface plasmom band gaps on metallic gratings," J. Appl. Phys. **79**(9), 7383 (1996).
21. S. Balci, A. Kocabas, C. Kocabas, and A. Aydinli, "Slowing surface plasmon polaritons on plasmonic coupled cavities by tuning grating grooves," Appl. Phys. Lett. **97**(13), 131103 (2010).
22. S. Mandal and D. Erickson, "Nanoscale optofluidic sensor arrays," Opt. Express **16**(3), 1623–1631 (2008).
23. N. Ganesh and B. T. Cunningham, "Photonic-crystal near-ultraviolet reflectance filters fabricated by nanoreplica molding," Appl. Phys. Lett. **88**(7), 071110 (2006).
24. A. M. Armani, R. P. Kulkarni, S. E. Fraser, R. C. Flagan, and K. J. Vahala, "Label-free, single-molecule detection with optical microcavities," Science **317**(5839), 783–787 (2007).
25. C. A. Barrios, K. B. Gylfason, B. Sánchez, A. Griol, H. Sohlström, M. Holgado, and R. Casquel, "Slot-waveguide biochemical sensor," Opt. Lett. **32**(21), 3080–3082 (2007).
26. W. Liang, Y. Huang, Y. Xu, R. K. Lee, and A. Yariv, "Highly sensitive fiber Bragg grating refractive index sensors," Appl. Phys. Lett. **86**(15), 151122 (2005).
27. G. M. Hwang, L. Pang, E. H. Mullen, and Y. Fainman, "Plasmonic sensing of biological analytes through nanoholes," IEEE Sens. J. **8**(12), 2074–2079 (2008).
28. E. M. Larsson, J. Alegret, M. Käll, and D. S. Sutherland, "Sensing characteristics of NIR localized surface plasmon resonances in gold nanorings for application as ultrasensitive biosensors," Nano Lett. **7**(5), 1256–1263 (2007).
29. G. A. Campbell and R. Mutharasan, "PEMC sensor's mass change sensitivity is 20 pg/Hz under liquid immersion," Biosens. Bioelectron. **22**(1), 35–41 (2006).
30. N. Ramakrishnan, T. Vamsi, A. Khan, H. B. Nemade, and R. P. Palathinkal, "Humidity sensor using NIPAAm nanogel as sensing medium in saw devices," Int. J. Nanosci. **10**(01n02), 259–262 (2011).
31. E. Popov, "Plasmon interactions in metallic gratings: ω- and k-minigaps and their connection with poles and zeros," Surf. Sci. **222**(2-3), 517–529 (1989).
32. F. Toigo, A. Marvin, V. Celli, and N. Hill, "Optical properties of rough surfaces: general theory and the small roughness limit," Phys. Rev. B **15**(12), 5618–5626 (1977).
33. R. Petit and M. Cadilhac, "Sur la diffraction d'une onde plane par un réseau infiniment conducteur," Acad. Sci., B **262**, 468 (1966) (in French).
34. A. Akhmanov, V. N. Seminogov, and V. I. Sokolov, "Light diffraction at corrugated surfaces," J. Exp. Theor. Phys. **93**, 1654 (1987) (in Russian).
35. V. N. Seminogov and V. I. Sokolov, "Influence of the nonmonochromaticity of the periodic relief of a surface on the effect of total suppression of the specular reflection of an s-polarized electromagnetic wave," Opt. Spectrosc. **68**, 50–53 (1990).
36. A. V. Nesterov-Müller, *Laser beams with axially symmetric polarisation*, (Schatura, 2000).
37. http://www.allresist.de/wEnglish/produkte/SonderanfertigungenExperimentalmuster/0041.php
38. RSoft DiffractMOD, "RSoft Design Group." *http://www.rsoftdesign.com*
39. U. Schröter and D. Heitmann, "Grating couplers for surface plasmons excited on thin metal films in the Kretschmann-Raether configuration," Phys. Rev. B **60**(7), 4992–4999 (1999).
40. J. Homola, I. Koudela, and S. S. Yee, "Surface plasmon resonance sensors based on diffraction gratings and prism couplers: sensitivity comparison," Sens. Actuators B Chem. **54**(1-2), 16–24 (1999).

1. Introduction

Recently the demand for powerful sensors for biochemical, chemical and biological molecular binding processes strongly increased. Biosensors nowadays must meet increased demanding requirements in terms of selectivity, sensitivity and resolution. In general terms, biosensing describes the detection of (usually) biological analytes by application of other biological substances – e.g. enzymes, antibodies, and peptides –, which are mostly immobilized to the sensors transducer surface [1,2]. Typical applications for biosensors include health screening, drug discovery, environmental monitoring, and food diagnostics, among many others [1–3].

Optical sensors play an important role in biosensing, due to their diverse distinct advantages, as e.g. their immunity to ambient electromagnetic fields, the potential for easy remote control, and the possibility to realize compact sensor systems on the micron-scale [1,4,5]. While labeled approaches apply the use of fluorescent markers, label-free schemes detect a change of a sensor's adjacent refractive index, induced by the binding events of the

#165521 - $15.00 USD Received 26 Mar 2012; revised 20 Apr 2012; accepted 20 Apr 2012; published 2 May 2012

analyte molecules of interest to the functionalized transducer surface. To detect these usually very small index changes, a strong interaction between the probing light and the analyte is required. In general terms, strong interaction leads to high sensitivity – namely to a strong sensor response to small index perturbations –, offering the possibility to even detect low affinity molecular binding events. An amplified interaction can be achieved with optical geometries utilizing metals. If distinct coupling preconditions are fulfilled, the excitation of charge density oscillations at a (dielectric) analyte/metal interface by light, results in the formation of surface plasmons (SPs) [6]. Due to their very high field overlap with the analyte, SPs show high sensitivity to refractive index changes, which are usually assessed by interrogating angular or spectral resonance features. Various designs of surface plasmon resonance (SPR) sensors have already been realized [7–9].

Another crucial parameter for a sensor's performance is the resolution – the ability to discriminate smallest signal changes. High resolution in optical sensor systems can be realized by a high number of "soft" measures, which involve optimization of the sensor's periphery – e.g. light source, detector, and signal processing. At a first stage one will work on the optimization of the sensor transducer itself. In SPR-based systems utilizing planar metallic surfaces, this signal optimization is limited to the dielectric functions of the involved materials and the thickness of the metal film. For further optimization, additional layers and geometries need to be introduced [10]. In all approaches, to the best of our knowledge, usually the coupling efficiency of the probing light to the SPs is optimized.

One promising approach for geometrical optimization of SPR-based structures is the utilization of periodically modulated metal surfaces [11,12]. These grating coupler based sensing schemes allow for easy fabrication and replication, even in large scale areas [12–14]. The working wavelength can be tuned continuously over a wide spectral range and narrow resonances can potentially be achieved, by adequate selection of the grating parameters and geometry.

The first observations of SPR features in the spectrum of diffracted light from these structures were made by Woods and reach back to 1902 [15]. Denoted as "diffraction anomalies", their occurrence triggered a broad discussion, with many scientists studying their origin [16,17]. Today, plasmonic grating structures offer a broad range of applications, including biosensing as one prominent example [7–9]. Their surface modulation can appear in complex geometries, with the SPRs usually being highly dependent of the involved geometrical parameters. A variety of theoretical approaches – utilizing e.g. Rayleigh theory [11,16] or rigorous coupling [18] – have been developed, to understand the physical mechanisms and to design SPR geometries towards various applications. One parameter turning out to play a crucial role in device design is the modulation depth, which is as well in the focus of the presented work. E.g. Baltog et al. demonstrated that the Raman efficiency in their grating structures is optimal for modulation depths around 50 nm [19]. Kitson et al. showed that the spectral position of plasmon band gaps highly depends on modulation [20], and Balci et al. verified that the plasmon group velocity and dispersion can be influenced by tuning the grating depth [21]. All these examples imply that there is a strong need for geometrical parameter optimization to achieve the optimal device performance.

Here we present a comprehensive design rule for SPR gratings in reflection mode, with focus on biosensing. By applying an analytical approach, based on Rayleigh theory, we introduce how grating periodicity and modulation depth for optimal coupling to SPs can be determined for any given grating geometry and design wavelength. Then we experimentally verify the design rule, for the example of gratings with sinusoidal surface modulation. In this experiment we furthermore present, how the analytically found grating modulation depth can be fine-tuned to achieve optimal signal discrimination, by seeking the optimal set of the SPR spectral width and the coupling efficiency. Assisted by numerical simulations, we introduce a benchmark factor γ_{OB}, which allows for this optimization, and which can be used to quantitatively assess the sensor performance. γ_{OB} can principally be applied to a broad range of sensor schemes utilizing resonance shifts, e.g. photonic crystal resonators [22,23],

#165521 - $15.00 USD Received 26 Mar 2012; revised 20 Apr 2012; accepted 20 Apr 2012; published 2 May 2012

whispering gallery mode resonators [24,25], fiber bragg-gratings [26], metallic transmission gratings [27], split rings [28], or even mechanical systems [29,30]. It allows benchmarking the sensor performance and optimizing signal resolution. This opens the possibility for direct comparison of sensing schemes based on different technologies.

2. Analytical method to estimate grating parameters for optimal SPR coupling efficiency

Our analysis is based on the Rayleigh hypothesis [11]. According to this hypothesis, diffracted electromagnetic fields can be constructed as Fourier sums that include the Fourier harmonics of a modulated diffractive interface in the form of Bloch vectors. This approach has been in the research focus of many authors [31,32] and was used by Tiogo et al. to derive an analytic description for the width of the SP band gap [32].The method is primarily valid in the case of gratings with small modulation (modulation depth <10% of the period) [33], although its applicability might be extended to gratings with [11].

The specific feature of our approach is that it uses the Rayleigh hypothesis to analyze the influence of arbitrary periodic surface modulations on diffraction fields in the case of resonant excitation of surface waves [34,35]. The sharp resonances enable to transform the infinite system of diffracted waves to a finite system for chosen resonant waves. This approach has been proved to be useful for searching for optimal resonant grating geometries and for physical interpretations of the observed resonances. Originally, this theory was developed to qualitatively understand the self-organization effects of materials melted by laser radiation [35]. Furthermore, it was used to calculate the geometric parameters of optical diffraction elements with high polarization selectivity [36]. Here, we will adapt this analytical approach to develop a design rule for SPR gratings for biosensing applications. The design goal is to find the geometrical parameters for maximum coupling of the incident light to selected SPs.

As well known, light with an electric field component perpendicular to a metallic surface relief (H-polarization) can excite SPs. Figure 1 depicts an arbitrary periodic medium with complex permittivity $\varepsilon = (n + im)^2$, irradiated by an H-polarized plane wave $E_{ix}(z,t) = E_i \exp(ikz - i\omega t)$, with $k = 2\pi n_{\text{cov}} / \lambda = \omega n_{\text{cov}} / c$, where k is the angular wave number, $n_{\text{cov}} = \left[\varepsilon_{\text{cov}}\right]^{1/2}$ the refractive index of the covering medium, ω the angular frequency, and c the vacuum wavelength.

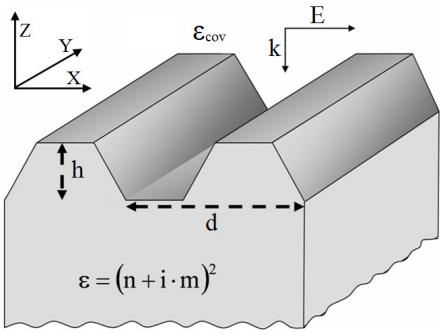

Fig. 1. Arbitrary grating relief (*d*: grating period, *h*: modulation depth, ε : dielectric permittivity of the grating material, ε_{cov} : dielectric permittivity of the cover material). The normally incident plane wave is polarized perpendicular to the stripes.

Considering the grating medium exhibiting periodicity along *x*, the surface being infinitely expanded along *y* (one-dimensional grating), and the interface centered at $z = 0$, the periodic function $f(x)$ can be developed in a Fourier series as

$$\mathrm{f(x)} = \sum_{\mathrm{p}=-\infty}^{\infty} \xi_p \exp(-ipgx), \qquad \xi_{-p} = \xi_p^*, \xi_0 = 0, \tag{1}$$

#165521 - $15.00 USD Received 26 Mar 2012; revised 20 Apr 2012; accepted 20 Apr 2012; published 2 May 2012

where ξ_p is the amplitude of the p^{th} order Fourier harmonics and $g = 2\pi / d$ the grating number, with the grating period d.

The total diffractive field in the cover medium can be developed in the Rayleigh series of plane waves [11,35]:

$$E = E_i \exp(ikz - i\omega t) + \sum_{p=-\infty}^{\infty} E_p \exp(ik_p x + \Gamma_p z - i\omega t), \tag{2}$$

with $k_p = -pg$, and $\Gamma_p = (k_p^2 - k^2)^{1/2}$, whereby $\mathrm{Re}(\Gamma_p) > 0$, if $-k_p > k$, $\mathrm{Im}(\Gamma_p) < 0$, if $-k_p < k$, and $p = [0, \pm 1, \pm 2, \pm 3, \pm 4]$. The value $p = 0$ corresponds to the mirror specular reflection. Note that the electric field vector of the diffractive field lays in the x-plane.

SPs appear along material interfaces for which $\varepsilon < -(n_{\mathrm{cov}})^2$ is valid. Considering slowly varying surface modulation ($k^2 f^2(x) << 1$, $\delta f(x) / \delta x << 1$) and using $|\varepsilon| >> |\varepsilon_{\mathrm{cov}}|$ as an approximation, the mirror reflected waves E_0 and the surface plasmon waves $E_{x,\pm 1}$ of the order $p = \pm 1$ are described according to

$$E_0 = \frac{(k - i\gamma_0)}{(k + i\gamma_0)} E_i - igE_1\xi_{-1} + igE_{-1}\xi_1, \tag{3}$$

$$E_{\pm 1} = \pm \frac{(kg(E_i - E_0)\xi_{\pm 1} \mp 2g^2 E_{\mp 1}\xi_{\pm 2})}{kT}, \tag{4}$$

$$T = T_0 + iT_1 = \frac{\sqrt{g^2 - k^2}}{k} - \beta_m - \sum_{\mathrm{p}=1,2,\pm 3,\pm 4\ldots} \frac{p^2 g^4}{k\Gamma_{(\mathrm{p}+1)}} \left|\xi_{\mathrm{p}}\right|^2 - i\beta_{\mathrm{n}}, \tag{5}$$

where $\beta_m = m / (m^2 + n^2)$, $\beta_n = n / (m^2 + n^2)$, $\gamma_0 = k(1 - \varepsilon)^{1/2} \approx (m - in) \cdot k$, and $\beta_m, \beta_n << 1$. The system of Eq. (3) and (4) is derived using boundary conditions and the Maxwell equations for the total electric field (Eq. (2)) and assuming the existence of sharp plasmonic resonances for surface waves. A detailed derivation of the system (3) – (4) is given in Ref [34].

Equations (3)–(5) can be interpreted as follows: The first term in Eq. (3) accounts Fresnel reflection of the incident radiation from the surface. The second and the third term correspond to scattering of the resonant waves E_1 and E_{-1} on harmonics ξ_1 and ξ_{-1} into Fresnel waves. The first term of Eq. (4) describes the generation of two resonant waves E_1 and E_{-1} on the harmonics $g \approx k$ with parameters ξ_1 and ξ_{-1} upon incidence of an H-polarized electromagnetic plane wave. The second term describes scattering between the resonant waves E_1 and E_{-1} on the Fourier harmonics of the relief with parameters ξ_2 and ξ_{-2}. The parameter T in Eq. (5) is the dispersion term and describes the dispersion of the surface waves at $T = 0$. The last term in Eq. (5) accounts to ohmic losses of the surface waves.

From Eq. (3)–(5), the expression for the reflection coefficient $R_\perp \equiv |E_0|^2 / |E_i|^2$ can be derived as

#165521 - $15.00 USD Received 26 Mar 2012; revised 20 Apr 2012; accepted 20 Apr 2012; published 2 May 2012

$$R_{\perp} = \frac{R_{\Phi}\Delta_{(-)}}{\Delta_{(+)}},\ R_{\Phi} = \left|\frac{(k - i\gamma_0)}{(k + i\gamma_0)}\right|^2,$$

$$\Delta_{(\pm)} = \left[k^2 T_0^2 - \beta_n k(\beta_n k \mp 2kg^2 |\xi_1|^2) - 4g^4 |\xi_2|^2\right]^2 \qquad (6)$$

$$+4\left[kT_0(\beta_n k \mp kg^2 |\xi_1|^2) \mp kg^4(\xi_1^{*2}\xi_2 + \xi_1^2\xi_2^*)\right]^2,$$

with the Fresnel reflection coefficient R_{Φ}. Assuming total suppression of the mirror reflected waves, the following conditions hold:

$$\begin{aligned} k^2 T_0^2 - \beta_n k(\beta_n k - 2kg^2 |\xi_1|^2) - 4g^4 |\xi_2|^2 &= 0, \\ kT_0(\beta_n k - kg^2 |\xi_1|^2) - kg^4(\xi_1^{*2}\xi_2 + \xi_1^2\xi_2^*) &= 0. \end{aligned} \qquad (7)$$

If the geometry of the relief is known, the Fourier components of the relief have the form $\xi_p = a_p h$. Here h is the modulation depth of the grating and a_p characterizes the surface profile. Inserting these expressions into Eq. (7), the optimum parameters for the period d_{opt} and the relief height h_{opt} can be calculated. Gratings with these parameters should theoretically convert the incident radiation by 100% into surface plasmons.

In practice, many grating geometries satisfy the condition $f(x) = f(x + d/2)$ corresponding to the case that all even harmonics of the relief Fourier series are equal to zero. Hence, assuming $\xi_2 = 0$, the preconditions for optimum SPR coupling become $g^2 |\xi|^2 = \beta_n / 2$ and $T_0 = 0$. These preconditions have the explicit form

$$B = \sqrt{((n_{\mathrm{cov}}\lambda / d)^2 - 1)} = \beta_m + B/2,\ B \equiv \sum_{p=1,2,\pm3,\pm4\ldots} \frac{p^2 \beta_n (\lambda / n_{\mathrm{cov}} d)^2}{\sqrt{(p+1)^2 (\lambda / n_{\mathrm{cov}} d)^2 - 1)}} \frac{|a_p|^2}{|a_1|^2}, \qquad (8)$$

$$g^2 h^2 = \frac{\beta_n}{2|a_1|^2}. \qquad (9)$$

Further simplification of these equations for $|\varepsilon| >> |\varepsilon_{\mathrm{cov}}|$ leads to expressions for the optimum period d_{opt} and optimum height h_{opt} of the grating:

$$d_{opt} = \frac{\lambda}{n_{\mathrm{cov}}(1 + (\beta_m + B/2)^2)},\ B \approx \beta_n \sum_{p=1,2,\pm3,\pm4\ldots} \frac{p^2}{\sqrt{(p+1)^2 - 1)}} \frac{|a_p|^2}{|a_1|^2}, \qquad (10)$$

$$h_{opt} = \frac{d_{opt}}{2\pi |a_1|} \sqrt{\frac{n}{2(m^2 + n^2)}}. \qquad (11)$$

Equation (10) and (11) are basic analytical solutions which can be used for a straight-forward design of metallic gratings for resonant excitation of surface plasmons. They connect the most important parameters as wavelength, grating height, period, grating profile, and permittivity.

Please note that the presented theory deals with plane waves. This approach is applicable, if the lateral size of the laser beam is significantly larger than the propagation length of surface plasmons. Otherwise beam size effects have to be taken into account.

#165521 - $15.00 USD Received 26 Mar 2012; revised 20 Apr 2012; accepted 20 Apr 2012; published 2 May 2012

3. Determination of the grating parameters for optimal resolution for the example of sinusoidal gratings

The analytical approach in section 2 offers an intuitive and flexible method to estimate the period and modulation depth for a selected grating geometry and design wavelength towards optimum SP coupling efficiency. In biosensing applications the expected SPR shift upon molecular binding to the sensor transducer surface will usually be very small. Hence, to establish the feasibility to detect very low molecular concentrations and low-affinity binding events, it is crucial to optimize resolution. In this paragraph, we will show how the analytically determined solution can be refined in order to find the grating's modulation depth for optimal resolution.

We chose one-dimensional sinusoidal gratings, as they allow for efficient tuning and optimization of the spectrally well-defined resonances. Additionally, the sinusoidal pattern can easily be described in Fourier space, opening the possibility for an intuitive demonstration of the analytical solution.

The samples were fabricated by two-beam laser interference lithography (LIL) at a working wavelength of 266 nm, using a negative-tone photoresist (*SX AR-N 4800/16*, *Allresist* [37]), spun on pre-cleaned 25 x 25 mm glass slides. The pre- and postbake parameters were chosen adequately to realize a low contrast system, allowing for direct transfer of the sinusoidal interference pattern into the photoresist. The prebake was performed on a hotplate at 80°C for 2 minutes. For the postbake 70°C was applied for 2 minutes. The exposure dosage was $64\,\mathrm{mJ/cm^2}$. Prebake, exposure and postbake parameters were kept constant for all samples. To achieve the various modulation depths, the dip development (developer X AR 600-54/3) was performed between 30 s (for shallowest modulation) and 40 s (for deepest modulation), followed by a nitrogen dry blow. After development a hardbake was performed at 110°C for 1 minute. The photoresist gratings were coated with 3 nm chromium by thermal evaporation, to promote silver adhesion. Subsequently, silver was thermally evaporated with a film thickness of 125 nm, to achieve full reflectivity. We realized gratings with a periodicity of 405 nm, hence the 0th order SPR appearing at ~578 nm with water as the covering medium.

The spectral interrogation of our samples was performed by using the optical characterization setup illustrated in Fig. 2. A fiber-coupled supercontinuum source (*Koheras SuperK Versa*), emitting from ~490 – 830 nm, was connected to a polarization controller and a polarizer, to generate TM-polarized (E-Field vector perpendicular to the grating lines) radiation. Via a beam splitter the polarized light was guided to the sample under normal incidence, having a spot diameter of ~1 mm. The sample acted as the backside of a custom-made flow box, which consisted of the sample (with the grating pointing inwards) and a counter glass slide, both separated from each other by a rubber ring, defining the chamber volume. This configuration was fixed with a polymer frame. The reflected broadband light beam was focused onto the end facet of an optical fiber and coupled into a fiber-coupled USB spectrometer (*Ocean Optics HR2000 +).*

#165521 - $15.00 USD Received 26 Mar 2012; revised 20 Apr 2012; accepted 20 Apr 2012; published 2 May 2012

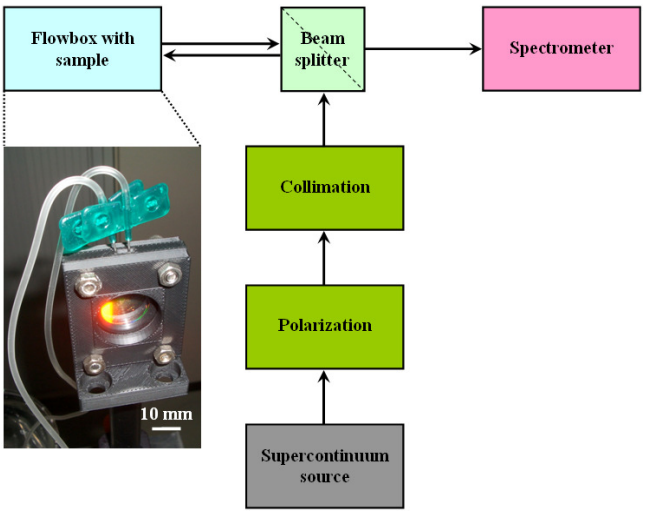

Fig. 2. Schematic principle of the optical characterization setup. The broadband radiation of a supercontinuum source is polarized and guided to the microfluidic chamber via a beam splitter. The light impinges the substrate under normal incidence. The reflected light passes the beam splitter anew and is spectrally investigated by a fiber-coupled spectrometer. The inset shows a photograph of the flowbox, in which the sensor sample acts as its back side.

In the case of a sinusoidal relief, all coefficients a_p in Eq. (10) with $p \neq 1$ are zero. Furthermore, a_1 and B become $1/4$ and $\beta_n/(3)^{1/2}$, respectively. The refractive index n_{cov} of the cover medium is set to 1.333 (water). Utilizing silver as the grating material and the SPR working wavelength of 578 nm $(\varepsilon = (0.0697 + i3.7645)^2)$, the grating parameters for optimal coupling efficiency are calculated to

$$d_{opt} = \frac{\lambda}{n_{\mathrm{cov}}(1+(\beta_m+\beta_n/2\sqrt{3})^2)} \approx 405 \text{ nm}, \tag{12}$$

$$h_{opt} = \frac{2d_{opt}}{\pi}\sqrt{\frac{n}{2(m^2+n^2)}} \approx 13 \text{ nm}. \tag{13}$$

Figure 3 depicts the simulated spectral behavior of the 0th order SPR, applying the above values for d, h, and n_{cov}. The simulation was performed utilizing the module *DiffractMod* of the commercially available software *Photonics Design Suite* from *RSoft*, which is based on rigorous coupled waveguide analysis (RCWA) [38]. For the wavelength dependency of ε for silver we used the data from [39]. The simulation result shows, that the analytically found solution, where a fixed ε was applied, is well-suitable to set the SPRs working wavelength to 578 nm.

#165521 - $15.00 USD Received 26 Mar 2012; revised 20 Apr 2012; accepted 20 Apr 2012; published 2 May 2012

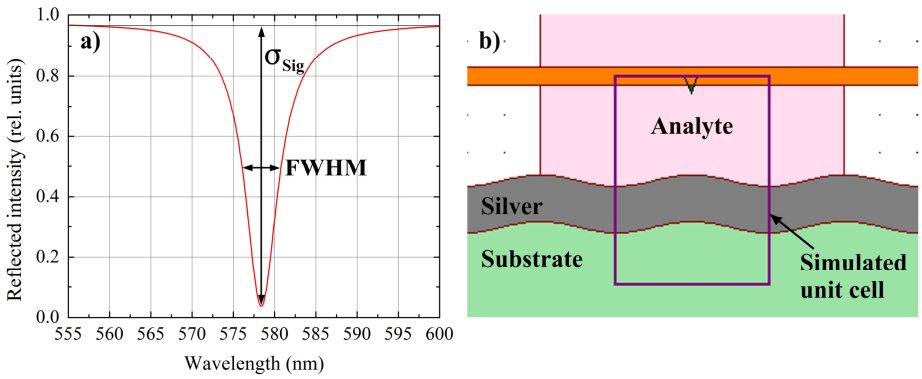

Fig. 3. (a) Numerically predicted reflection spectrum of the 0th order SPR on a sinusoidal silver surface (Grating period: 405 nm, modulation depth: 13 nm, silver film thickness: 125 nm), simulated by RCWA. The full-width-half-maximum (FWHM) and the coupling strength σ_{Sig} are extracted by Lorentzian fitting. (b) Schematic illustration of the sensor geometry and the RCWA unit cell.

To determine the influence of the grating modulation on the resonance profile we repeated the simulation procedure for gradually increasing modulation depth and derived the respective SPR full-width-half-maximum (FWHM) and coupling strength σ_{Sig} (depth of the SPR) (both parameters highlighted exemplarily in Fig. 3(a)), by applying Lorentzian fitting. Lorentzian fitting was as well performed on the experimental spectra. The relationship is elucidated in Fig. 4(a) and (b), respectively. While the FWHM increases significantly with growing modulation depth, the coupling efficiency experiences a maximum at around 16 nm. The small deviation of the analytical result $h_{opt} = 13\,\mathrm{nm}$ from the simulated value can be accounted due to the assumption of $|\varepsilon| >> |\varepsilon_{\mathrm{cov}}|$ taken for the derivation of Eq. (12). Maximum coupling strength is usually comprehended as one major sensor design optimum – in SPR sensing as well as in sensing in general –, as the strongest sensor signal is apparent here. Alternatively, to seek the optimal sensor resolution, one might optimize towards smallest resonance line width. Figure 4 implies that in the present case both optimization scenarios result in different target modulation depths: While the abovementioned case for optimal coupling would presume a modulation depth of $\sim 16\,\mathrm{nm}$, the smallest resolution would be achieved for the shallowest possible grating. In practice, this choice would not be desirable, as on the one hand, the coupling strength becomes negligibly small, and on the other hand, these grating geometries are very difficult to fabricate. Figure 4 furthermore shows, that our experimental results agree well with the numerically predicted signal behavior. In comparison to the perfectly shaped sinus accounted in the simulations, we assume that the experimentally observed in average wider FWHM and reduced coupling efficiency are a result of the roughness of the silver film (Fig. 5), inducing additional optical losses. The average RMS (root mean square) silver film roughness was 4.3 nm, with local average maximum values of $\sim 41\,\mathrm{nm}$, measured by atomic force microscope (AFM).

#165521 - $15.00 USD Received 26 Mar 2012; revised 20 Apr 2012; accepted 20 Apr 2012; published 2 May 2012

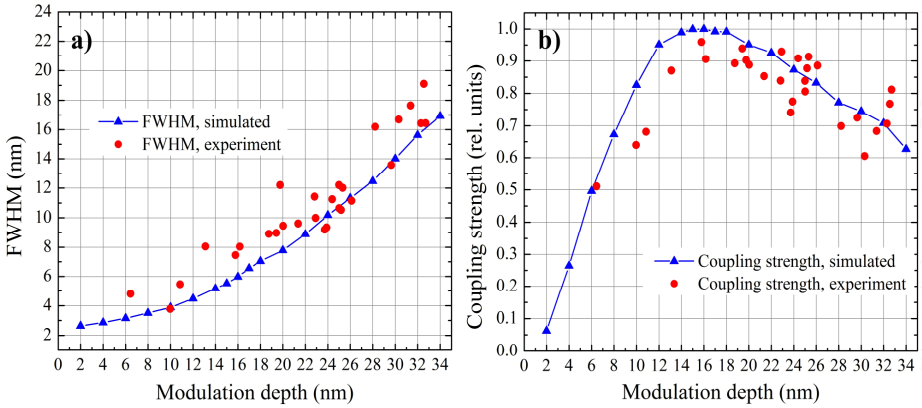

Fig. 4. Simulated (blue triangles) and experimentally observed (red dots) behavior of the (a) SPR full-width-half-maximum (FWHM) and (b) the SPR coupling efficiency. While the FWHM increases with increasing grating modulation depth, the coupling strength σ_{Sig} experiences a maximum for a modulation depth of around 16 nm. Due to the roughness of the silver film, the experimental results are loss-afflicted (wider FWHM and lower coupling efficiency, than numerically predicted).

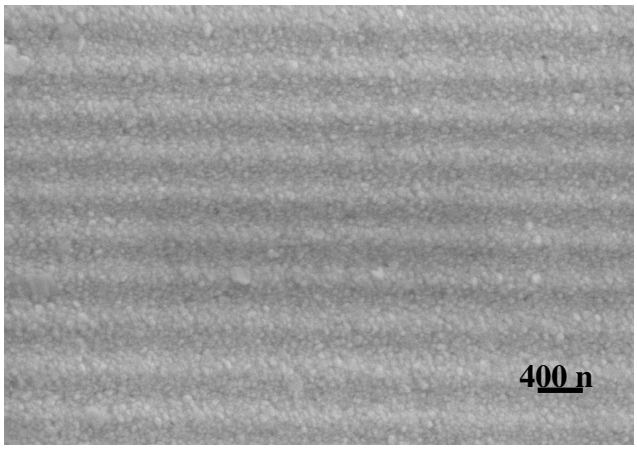

Fig. 5. SEM image of the sinusoidal silver surface of a fabricated sensor transducer. The roughness of the silver is induced by the inherent nature of the thermal evaporation process, and results in additional optical losses. In the present optical characterization experiments, the roughness lead to an increased sensitivity, in comparison to a perfectly smooth sinus, as the silver surfaces exhibits caverns and cracks, which the analyte can penetrate. The average RMS roughness was measured by AFM to 4.3 nm, with local maximum roughness values of ~41 nm,

As the signal resolution strongly depends on the overall resonance shape, one needs to find a suitable measure to assess its impact on the sensor performance. A steep and narrow resonance resulting in a large relative signal change for small refractive index change is required. To address this problem, we introduce an assessment factor γ_{OB}, which we define to

$$\gamma_{OB} = \frac{\sigma_{Sig}}{FWHM}. \tag{14}$$

Figure 6(a) depicts the calculated γ_{OB}, using the simulated values from Fig. 4. Interestingly, the modulation depth for optimal γ_{OB} is significantly different from the values obtained by isolated optimization of either resolution or coupling efficiency. The sole

#165521 - $15.00 USD Received 26 Mar 2012; revised 20 Apr 2012; accepted 20 Apr 2012; published 2 May 2012

optimization of the coupling strength σ_{Sig} would lead to a modulation depth of 16 nm. However, γ_{OB} indicates that the grating sensor resolution can significantly be increased by $\sim 27\%$, if the the grating depth is chosen to 10 nm ($\rightarrow \gamma_{OB} \approx 0.213\,\mathrm{nm}^{-1}$). Furthermore, a comparison of the numerically achieved γ_{OB} with the values extracted from the experiments shows that the performance of the fabricated sensors increasingly deviates from the predicted values for decreasing modulation depth. This effect can be explained by the quality of the silver film, having a higher impact on the performance worsening on shallow gratings, as the surface roughness represents a stronger relative disturbance here. Hence, we assume that γ_{OB} can as well be used to assess grating quality parameters, as optical losses due to surface roughness of the metal film in present case. Figure 6(b) elucidates that the factor γ_{OB} actually offers an intuitive possibility to assess the grating parameter configuration for optimal signal resolution. At maximum γ_{OB} the side slopes of the investigated SPR become steepest, allowing for best signal discrimination.

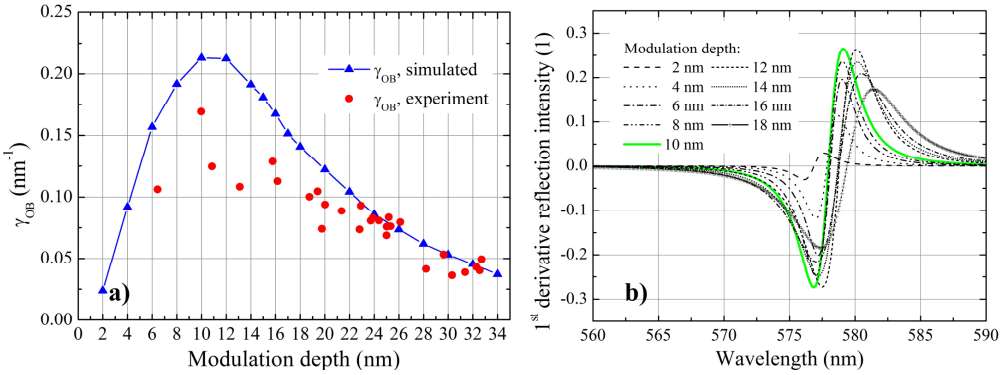

Fig. 6. (a) Calculated (blue triangles) and experimentally assessed benchmark factor γ_{OB} as a function of the grating modulation depth. A comparison elucidates that especially for shallower gratings the roughness of the silver film results in reduced signal discrimination. (b) First derivative of the numerically predicted spectral signal of the investigated SPRs for different modulation depth. At maximum γ_{OB} highest signal discrimination is achieved, as the side slopes of the resonance become steepest.

In [40] the authors propose a useful benchmark factor χ to assess the performance of their SPR sensors. This factor is defined by $\chi = S / w$ and allows for a direct comparison of the sensitivity of planar and periodically modulated transducer surfaces, assessing the predicted SPR shift and line width. Here, S is the sensitivity; the FWHM is defined by w. This formal definition of χ implies that an optimization towards optimal coupling strength is presumed ($\sigma_{Sig} = 1$). We think it is reasonable to expand this factor by the coupling efficiency, to obtain the ability to further optimize sensors towards optimal resolution:

$$\chi_{\mathrm{exp}} = \frac{S \cdot \sigma_{Sig}}{w} = \frac{S \cdot \sigma_{Sig}}{FWHM} = S \cdot \gamma_{OB}. \qquad (15)$$

Figure 7 shows the numerical prediction and the experimentally observed χ_{exp} for our investigated sinusoidal SPR gratings. By sweeping the analyte refractive index in distinct steps, the sensitivity was predicted to $\sim 418\,\mathrm{nm/RIU}$ (RIU: Refractive index unit). In the present investigated regime (2 – 34 nm), the sensitivity showed no dependency on the modulation depth. Experimentally, the index sweep was realized by exposing the sensors to various concentration mixtures of isopropylic alcohol (IPA) in distilled water (Fig. 8). Here,

#165521 - $15.00 USD Received 26 Mar 2012; revised 20 Apr 2012; accepted 20 Apr 2012; published 2 May 2012

we observed a modulation-independent sensitivity averaging around $\sim 630\,\mathrm{nm/RIU}$. We assume this higher sensitivity arises from the surface roughness of our fabricated silver surfaces. Due to this roughness, the sensor surfaces substantially exhibit cracks and caverns, which can be filled by the fluidic analyte, leading to a certain penetration of the analyte into the silver film, and furthermore give rise to local field enhancement, increasing the interaction between SPR and analyte. Interestingly, the reduced signal resolution due to the silver roughness is compensated by the simultaneously occurring sensitivity increase.

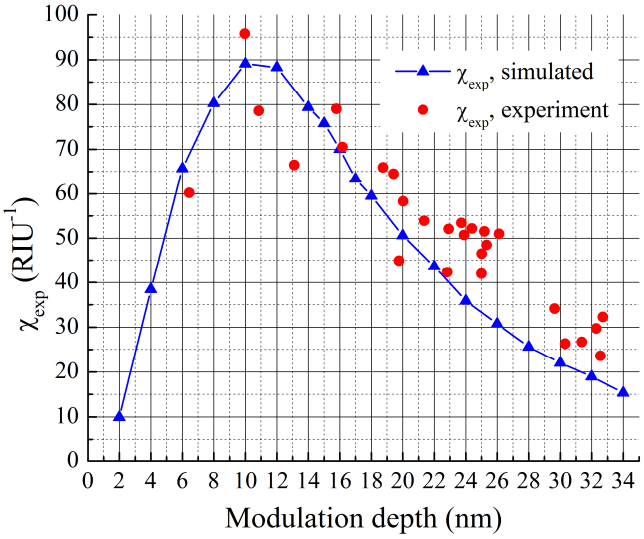

Fig. 7. Calculated (blue triangles) and experimentally assessed benchmark factor χ_{exp}, plotted over the grating modulation depth.

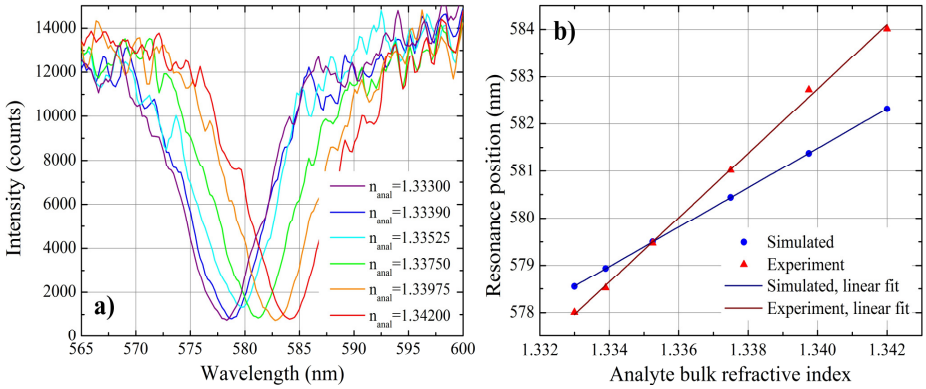

Fig. 8. (a) Exemplary experimental SPR shift during exposure of the grating surface to IPA/H_2O mixtures with various refractive indexes (Grating parameters: $d = 405$ nm, $h = 19.5$ nm, silver film thickness = 125 nm). (b) Comparison of the resonance shift in (a) with the shift numerically expected by RCWA simulation. The higher sensitivity achieved by experiment ($682.36\,\mathrm{nm/RIU}$ 682.36 nm/RIU, simulated value: $417.97\,\mathrm{nm/RIU}$) are attributed to the roughness of the silver film.

4. Conclusion

In conclusion, we propose a novel design rule to optimize plasmonic grating structures for refractive index sensing, with applications e.g. in biosensing. The design rule starts with an

#165521 - $15.00 USD Received 26 Mar 2012; revised 20 Apr 2012; accepted 20 Apr 2012; published 2 May 2012

analytical approach to estimate the grating period and modulation depth for optimal coupling efficiency of the probing light to the supported surface plasmon resonances. As the gratings are described by their Fourier components, the analysis can be applied on arbitrary grating geometries. For the example of sinusoidal gratings, fabricated by laser interference lithography, we experimentally demonstrate how the surface modulation depth can be furthermore optimized, to achieve the highest possible signal discrimination. Assisted by numerical simulations, we propose an assessment factor γ_{OB} to optimize the sensing performance. This factor takes into account coupling efficiency and FWHM of the observed surface plasmon resonances, and enables for the determination of the grating depth for their best set, to achieve global optimum signal discrimination. The application of γ_{OB} to the investigated sinusoidal gratings shows that the achievable signal discrimination can be higher than those obtained from existing optimization scenarios, where either coupling strength or FWHM are optimized individually. The factor γ_{OB} may be applied to a broad range of other sensing device utilizing resonance shifts, e.g. resonators based on photonic crystals or whispering gallery modes, metallic transmission gratings or fiber bragg-gratings, split rings, or even mechanical systems. Thus it can be a powerful tool for benchmarking the sensing performance of different sensor technologies.

Acknowledgement

Uwe Bog acknowledges the financial support by the Karlsruhe School of Optics and Photonics (KSOP). Timo Mappes' Young Investigator Group YIG 08 received financial support from the 'Concept for the Future' of Karlsruhe Institute of Technology within the framework of the German Excellence Initiative. This work has been supported by the DFG Research Center for Functional Nanostructures (CFN) Karlsruhe and was partly carried out with the support of the Karlsruhe Nano Micro Facility (KNMF, www.kmf.kit.edu), a Helmholtz Research Infrastructure at Karlsruhe Institute of Technology (KIT, www.kit.edu).

#165521 - $15.00 USD Received 26 Mar 2012; revised 20 Apr 2012; accepted 20 Apr 2012; published 2 May 2012